Songklanakarin J. Sci. Technol.
42 (4), 844-849, Jul. - Aug. 2020

http://www.sjst.psu.ac.th

Original Article

2D electrical resistivity tomography (ERT) method to delineate coal seams: Case studies on lignite and anthracite

Khamvanh Phengnaone[1], Rungroj Arjwech[1*], and Mark Everett[2]

[1] *Department of Geotechnology, Faculty of Technology, Khon Kaen University, Mueang, Khon Kaen, 40002 Thailand*

[2] *Department of Geology and Geophysics, Texas A&M University, College Station, Texas, 77843 United States of America*

Received: 26 May 2018; Revised: 2 January 2019; Accepted: 6 May 2019

Abstract

The 2D electrical resistivity tomography method was used to study the geometry of coal seams at two sites that differ in the local geological setting and type of coal. One site contains a lignite seam whereas the other contains an anthracite seam. The coal seam resistivity signatures were determined and the results were compared between the two study sites. The interpreted 2D resistivity tomograms showed that the lignite seam cannot be distinguished from the surrounding host rocks but the anthracite seam is clearly associated with high resistivity values up to 100 Ωm with respect to the low-resistivity background of shale. The type and age of coal affects the porosity and water saturation. Increases in these two parameters reduce the bulk resistivity of the formation. Type, age, and fluid content are important factors that determine the resistivity contrast of a coal seam with the surrounding rocks.

Keywords: electrical resistivity tomography (ERT), lignite, anthracite

1. Introduction

Coal is a major energy resource worldwide for electricity generation (Schnapp & Smith, 2012). Its exploitation contributes about 20% of Thailand's energy needs and that amount is expected to increase in the future (Schmollinger, 2018). In Lao PDR, coal energy supplied about 0.15% of the country's total energy needs in 2010 but the contribution from coal increased to 15.6% in 2015. The demand for coal everywhere is on the rise (Kouphokham, 2013). Besides electricity generation, coal is also used as fuel in other commercial and industrial processes such as cement production, metal smelting, and in the food industry (Schnapp & Smith, 2012).

Geophysical methods have long been used for coal exploration. The use of non-invasive geophysics is cost-effective and serves as an excellent complement to conventional geotechnical testing (Anderson, Hoover, & Sirles, 2008; Arjwech *et al.*, 2013; Arjwech & Everett, 2015). The results of geophysics exploration when combined with drill-hole data enables reliable coal mapping for exploration and exploitation (Afonso, 2014; Hatherly, 2013). It is advantageous to perform geophysical prospecting before the coal mining begins (Lei, 2015).

The electrical resistivity survey method was first developed in the early 1900's. It was used for coal investigations as early as 1934 (Ewing, Crary, Peoples, & Peoples, 1936; Tselentis & Paraskevopoulos, 2002). Today, multi-electrode resistivity systems comprise an advanced technology system that is used for mapping a subsurface electrical resistivity structure in two and three dimensions (Dahlin, 2001). Some studies (Singh, Singh K, Lokhande, & Prakash, 2004; Verma, Bandopadhyay, & Bhuin, 1982; Wu, Yang, & Tan, 2016) have demonstrated that the electrical resistivity tomography (ERT) survey method can successfully be used to study coal deposits. Generally, coal has a high

*Corresponding author
Email address: rungroj@kku.ac.th

electrical resistivity with respect to the lower values of the surrounding formations (Singh, Singh, Lokhande, & Prakash, 2004). Coal resistivity values vary from a few hundred to a few thousand ohm-meters (Ωm) depending on the geological setting (Hatherly, 2013; Verma & Bhuin, 1979). If coal has no porosity and is measured on a dry state, the expected resistivity is over a million Ωm (Hilchie, 1982). Resistivity values decay exponentially with an increase in the percentage of water saturation (Shreeman & Mukhdeo, 1993; Verma, Bhuin, & Handu, 2007). The bulk resistivity measured from core samples decreases as the temperature rises from 0 to 80 °C but sharply increases as the temperature rises from 80 to 180 °C (Shreeman & Mukhdeo, 1993).

In this study the ERT survey method was used to investigate coal seams at two sites that have different geological conditions and coal types. This study characterizes and contrasts the resistivity signatures of the two coal seams.

2. Site Location and Geological Setting

Two coal sites were selected where the geology has previously been studied such that the depth and thickness of the coal seams are known. At site A, an outcrop of the coal seam is exposed along a road cut on Highway 2216 in Nam Nao District, Phetchabun Province, Thailand. The exposed outcrop is ~160 m long. The coal-bearing rocks belong to the Huai Hin Lat Formation of the Upper Triassic age (Figures 1 and 2). The coal-bearing unit consists predominantly of calcareous mudstone intercalated with siltstone, lignite, and calcareous mudstone. From the lithological logs, the overlain calcareous mudstone and lignite beds are highly weathered (Figure 3). The thickness of the lignite layer is ~5 m (Boonnarong, Wannakomol, Qinglai, & Chonglakmani, 2016; Chonglakmani & Sattayarak, 1978).

Site B, is located in Sangthong District, Vientiane Province, Laos PRD, where coal has long been mined. The coal-bearing formation is found in association with rocks of the Upper Carboniferous to Lower Permian age. The coal is identified as anthracite and occurs in units of 1–15 m thickness. From the lithological logs recorded at the quarry, the anthracite is overlain by topsoil and underlain by intercalated thin-bedded shale (Figures 3, 4, and 5).

3. Methodology

Four and five profiles at Site A and Site B, respectively, were surveyed in August 2017. One profile could be deployed parallel to the face of the road cut and query. Therefore, only one ERT profile from each site is presented in this paper. Data acquisition was carried out on the ground surface over the known coal seams. The profile in each case was located about 15 m away from the rim of the road cut exposing the lignite and the anthracite quarry. This choice of profile location was made in an attempt to minimize the error caused by the presence of the nearby excavation. It is well-known that significant 3-D resistivity structures that are located off the ERT profile line can influence a tomographic reconstruction. The reason is that the electric current that flows in the Earth between the injection and collection electrodes is not confined to the vertical half-plane passing through the line joining these two electrodes.

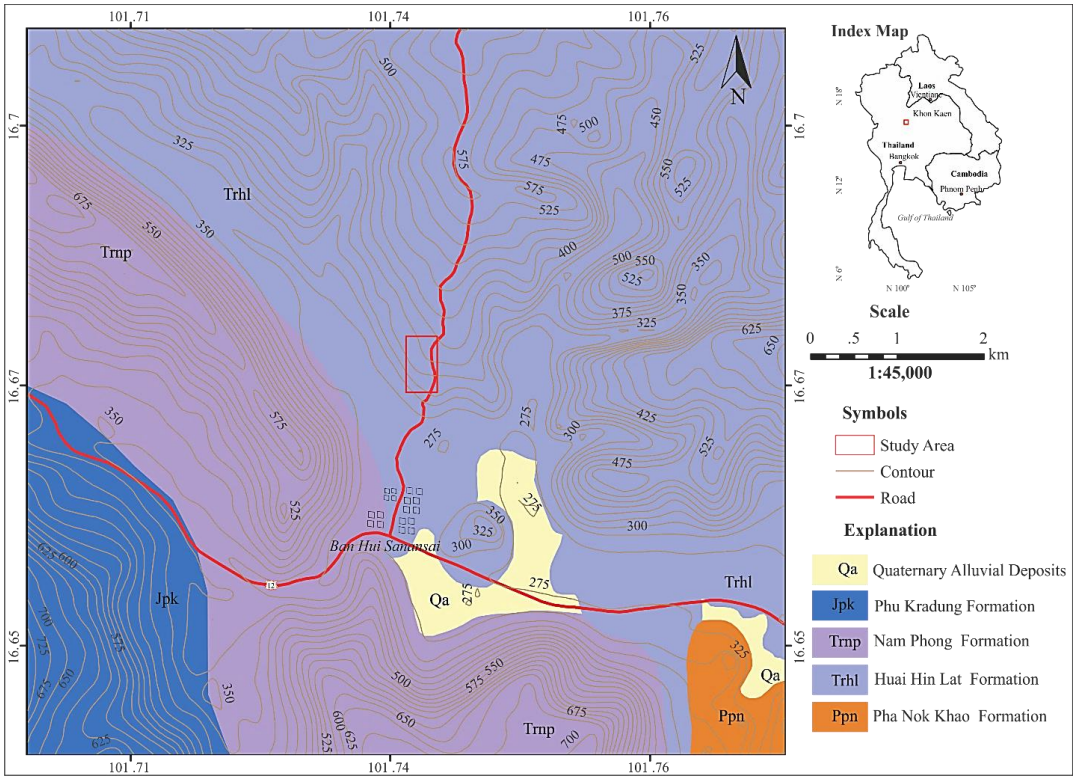

Figure 1. Geologic map of study site A (Department of Mineral Resources, 2000).

Figure 2. Lignite exposed along Highway 2216, Thailand, site A.

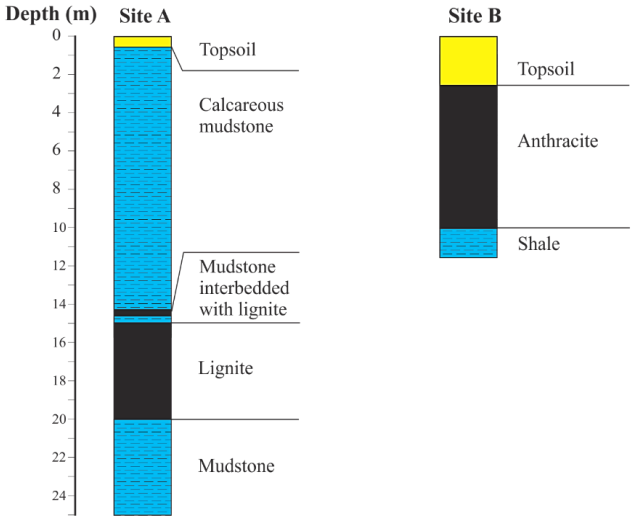

Figure 3. Stratigraphic columns of study site A and site B.

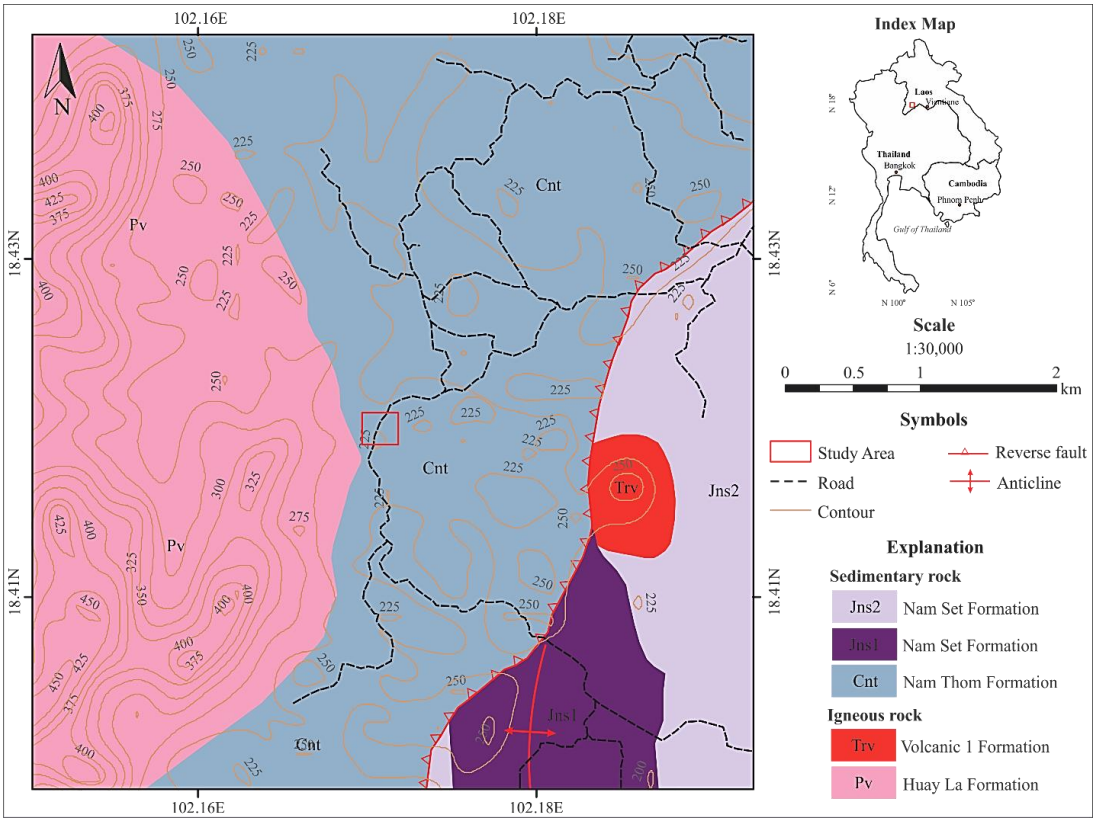

Figure 4. Map of study site B (Paphawin, Ukrit, & Warodom, 2012).

Figure 5. Anthracite was mined in Laos, site B.

At site A, a 2D ERT data set was collected using SYSCAL PRO by an IRIS Instrument (www.iris-instruments.com). The survey was conducted with Wenner-Schlumberger electrode configurations of 72 electrodes at 2.5 m spacing. The total length of survey profile was thus 177.5 m.

At site B, a 2D ERT data set was collected with the SuperSting^{TM} R8/IP multi-channel imaging system (www.agiusa.com) using a linear array of 48 steel electrodes. Wenner-Schlumberger electrode configurations were again selected with 3 m electrode spacing, yielding a total profile length of 141 m. Setting the parameters, such as injecting time and electrode array, on the command file were optimized as close as possible to make sure that different types of equipment had little effect on the measured data.

The ERT data were analyzed using the RES2DINV (www.geotomosoft.com) program for 2D apparent-resistivity pseudosection plotting, data editing, and inversion. The inversion algorithm is described quite well in Yang (1999) and Loke and Barker (1996). The coal boundaries interpreted on the resistivity tomograms were compared with the available lithological log information and the known geology of the sites.

4. Results

Figure 6a shows the inversion result, or ERT tomogram, at site A. The maximum depth of penetration was ~40 m at the middle of the profile, with a shallower penetration depth towards the ends of the profile. After six

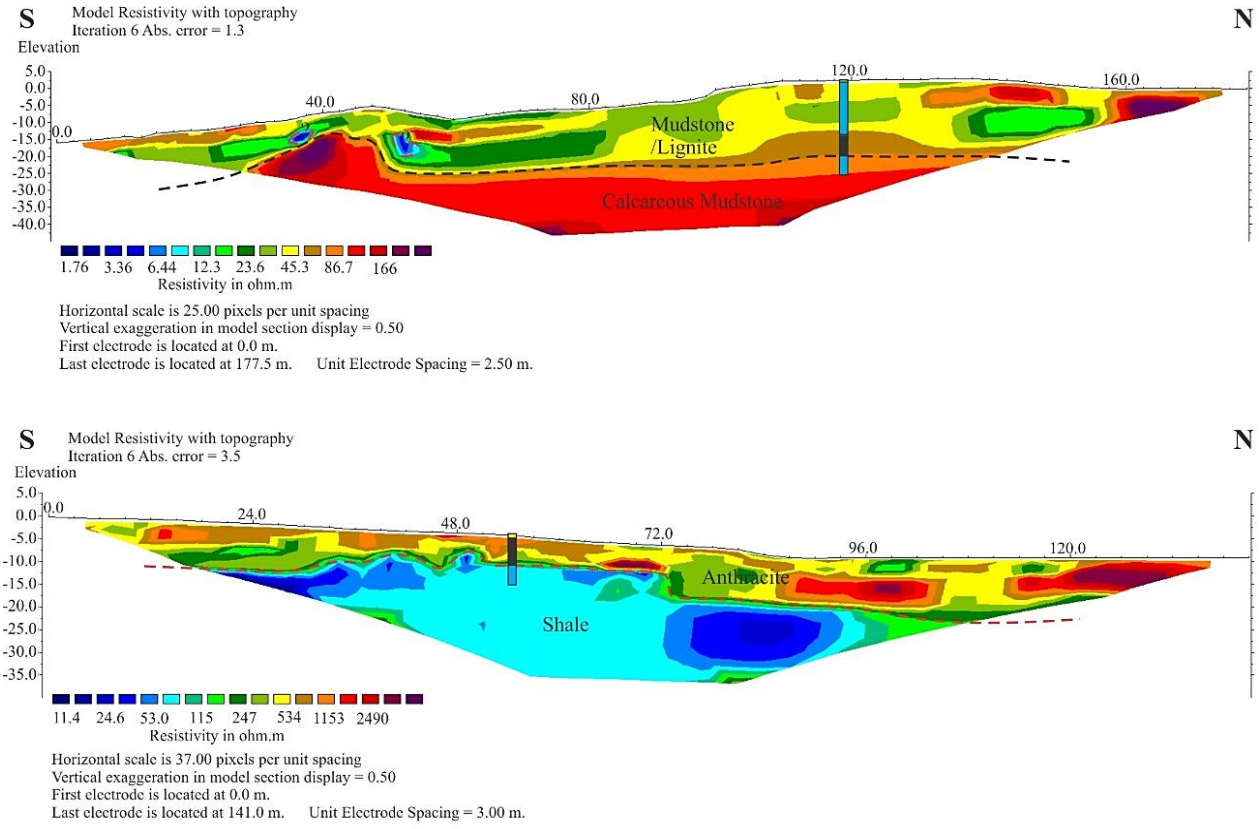

Figure 6. Inversion images of site A and site B with stratigraphic columns.

iterations, the inversion process converged with a root mean square (RMS) misfit of 1.3. A heterogeneous zone of relatively low resistivity (<100 Ωm) is evident along the entire length of the profile from the surface to a depth of ~25 m. The surface layer, which is marked by the black dashed line in Figure 6a, is interpreted as calcareous mudstone intercalated with siltstone and lignite. The resistivity tomogram was not consistent with the lithological log, which for convenience is superimposed on the tomogram at position 120 m from the start of the profile. The coal seam noted in the log is distinct and located at a 15–20 m depth. However, the lignite clearly does not produce a distinctive layer at this depth in the resistivity tomogram. Samanlangi (2018), who also used ERT, found lignite resistivity to fall within the range of 70–200 Ωm which is quite consistent with our results, and explains why the lignite zone might not appear as a distinct layer on the tomogram. The relatively homogeneous zone of higher resistivity (>100 Ωm) extending from the beginning to the end of the profile below ~25 m depth is interpreted as calcareous mudstone. The depth to the calcareous mudstone appears to be anomalously shallow in the interval about 30–45 m along the profile. The cause of this anomalous shallowing of the calcareous mudstone is not known but may represent a disruption in the continuity of the lignite bed.

Figure 6b shows the resistivity tomogram at site B. The maximum depth of penetration was ~30 m at the middle of the profile. After five iterations, the inversion process converged with a RMS misfit of 3.5. A heterogeneous but distinctive layer of high resistivity (>100 Ωm) was found near the surface along the entire length of the profile. This layer, which is marked by the red dashed line in Figure 6b, is interpreted to be caused by the presence of anthracite, consistent with the exposure in the nearby quarry. Generally, coal resistivity increases with organic content (Afonso, 2014) with anthracite values exceeding 100–1000 Ωm in some cases. The appearance of such high resistivity is readily associated with anthracite. However, a topsoil layer is observed in the quarry and also identified on the lithological log. The latter is superimposed for convenience on the tomogram at the location ~54 m from the start of the profile. The topsoil layer cannot be resolved in the resistivity tomogram. The lower resistivity (<100 Ωm) zone extending along the bottom of the tomogram is interpreted to be due to weathered shale. Shale fragments were observed in the lithological log of the drilled borehole at these depths and they were also noticed to be scattered about on the quarry floor.

5. Discussion

In general, earth resistivity is related to various soil and rock properties such as moisture content, porosity, fracture density, mass density, degree of water saturation, and compaction. The most important conductive mechanism in rocks is electrolytic with electric current flow taking place through the fluid-filled connected pore space. In this study the geological setting of the coal seams varies considerably between the two surveyed areas. Many factors affect the resistivity contrast between the coal and the surrounding rock formations. At site A, weathered mudstone and the high moisture content of the lignite cause a relatively low resistivity contrast that was not evident on the resistivity tomogram. At this site, lignite overlies a calcareous mudstone bed. At site B, the anthracite was hard, compact, and contained less moisture. Therefore, it had a higher resistivity than the underlying weathered shale. Anthracite has a more distinctive resistivity signature than lignite. Since anthracite is a harder coal than lignite from a geological perspective, anthracite should exhibit a significantly larger resistivity in contrast to the background host sediments than lignite. The age of the coal, i.e. younger lignite (Upper Triassic) and older anthracite (Carboniferous), is also an important factor in determining the resistivity. The age affects the degree of compaction and the magnitude of coal porosity. Anthracite typically has higher resistivity values than lignite because lignite is usually more porous and has higher water content. Fractures were not observed on either of the resistivity tomograms. This is consistent with the field observation that only minor fractures appeared in both outcrops.

6. Conclusions

The multi-electrode 2D ERT method was used to study coal seams at one site in Thailand (lignite) and one site in Lao PRD (anthracite) that differed in geological settings and types of coal. The study characterized and compared the coal resistivity signatures at the two sites. It was concluded that the lignite bed at site A could be delineated due to the low resistivity contrast between the lignite and the surrounding rocks. The anthracite seam at site B could be better identified and delineated as a high resistivity zone overlying the lower-resistivity layer of shale. Porosity and moisture content play important roles in the successful application of this survey method. The type and age of coal has an important effect on porosity, such that water saturation reduces the resistivity of the formation. These are important factors that affect their resistivity contrasts with the surrounding rocks and, ultimately, the detectability of a coal seam using the ERT method.

Acknowledgements

This work was financially supported by Department of Geotechnology, Faculty of Technology and Graduate School, Khon Kean University.

References

Afonso, J. M. (2014). *Electrical resistivity measurements in coal: Assessment of coal-bed methane content, reserves and coal permeability* (Doctoral thesis, The University of Leicester, Leicester, England).

Anderson, N., Hoover, R., & Sirles, P. (2008). *Geophysical methods commonly employed for geotechnical site characterization*. Transportation Research Broad of the National Academies. Retrieved from http://www.trb.org/Publications/Blurbs/160352.aspx

Arjwech, R., & Everett, M. E. (2015). Application of 2D electrical resistivity tomography to engineering projects: Three case studies. *Songklanakarin Journal of Science and Technology*, *37*(6), 675-681.

Arjwech, R., Everett, M., Briaud, J. L., Hurlebaus, S., Medina-Cetina, Z., Tucker, S., & Yosefpour, N. (2013). Electrical resistivity imaging of unknown bridge foundations. *Near Surface Geophysics*, *11*, 591-598.

Boonnarong, A., Wannakomol, A., Qinglai, F., & Chonglakmani, C. (2016). Paleoproductivity and paleoredox condition of the Huai Hin Lat formation in Northeastern Thailand. *Journal of Earth Science*, *27*, 350-364.

Chonglakmani, C., & Sattayarak, N. (1978). Stratigraphy of Huai Hin Lat formation (Upper Triassic) in Northeastern Thailand. *Proceedings of the Third Regional Conference on Geology and Mineralogy Resources of Southeast Asia*, 739-762.

Dahlin, T. (2001). The development of DC resistivity imaging techniques. *Computers and Geosciences*, *27*, 1019-1029.

Department of Mineral Resources. (2000). Geological map of Thailand, scale 1:250000. Bureau of Geological Survey, Department of Mineral Resources, Bangkok, Thailand.

Ewing, M. A., Crary, A. P., Peoples J. W., & Peoples, J. A. (1936). Prospecting for anthracite by the earth resistivity method, transactions of the American of Mining and Metallurgical Engineers. *Coal Division*, *119*, 43-483.

Hatherly, P. (2013). Overview on the application of geophysics in coal mining. *International Journal of Coal Geology*, *114*, 74–84.

Hilchie, D. W. (1982). *Applied openhole log interpretation (for geologists and engineers)*. Golden, CO: Doug las W. Hilchie.

Kouphokham, K. (2013). Analysis on energy saving potential in East Asia region, ERIA Research project report 2011, No. 18. Retrieved from https://www.eria.org/RPR-2011-18.pdf

Lei, Y. (2015). Application of geophysical technique in the coal mining. *International Journal of Online Engineering*, *11*(7), 11-13.

Loke, M. H., & Barker, R. D. (1996). Rapid least-squares inversion of apparent resistivity pseudosections by a quasi-newton method. *Geophysical Prospecting*, *44*, 131-152.

Paphawin, T., Ukrit, M., & Warodom, K. (2012). *Coal bearing rock, crossed-section, coal exploration of Ban Koua, Sang Thong and Hin Heoup, Vientian.* Bangkok, Thailand: Lao Metal Industry Company Limited.

Samanlangi, A. I. (2018). Coal layer identification using electrical resistivity imaging method in Sinjai area south Sulawesi. *Journal of Physics Conference Series*, *979*, 012048.

Schmollinger, C. (2018). Thailand plans to increase coal use in power generation – minister. Retrieved from https://www.reuters.com/article/india-ief-thailand/thailand-plans-to-increase-coal-use-in-power-generation-minister-idUSL3N1RP1TV

Schnapp, R., & Smith, J. (2012). *Coal information*. Paris, France: International Energy Agency.

Shreeman, N. T., & Mukhdeo. (1993). Measurement of electrical resistivity of coal samples. *Fuel*, *72*(8), 1099-1102.

Singh, K. K., Singh, K. B., Lokhande, R. D., & Prakash, A. (2004). Multielectrode resistivity imaging technique for the study of coal seam. *Journal of Scientific & Industrial Research*, *63*, 927-930.

Tselentis, G. A., & Paraskevopoulos, P. (2002). Application of a high-resolution seismic investigation in a Greek coal mine. *Geophysic*, *67*, 50-59.

Verma, R. K., Bandopadhyay, T. K., & Bhuin, N. C. (1982). Use of electrical resistivity methods for study of coal seams in parts of the Jharia Coalfield, India. *Geophysical Prospecting*, *30*, 115-126.

Verma, R. K., & Bhuin, N. C. (1979). Use of electrical resistivity methods for study of coal seams in parts of the Jharia Coalfield, India. *Geoexploration*, *17*(2), 163-176.

Verma, R. K., Bhuin, N. C., & Handu, S. K. (2007). Study of the resistivity of coal seams of the Jharia coalfield, India. *Energy Sources*, *6*(4), 273-291.

Wu, G., Yang, G., & Tan, H. (2016). Mapping coalmine goaf using transient electromagnetic method and high density resistivity method in Ordos City, China. *Geodesy and Geodynamics*, *7*(5), 340-347.

Yang, X. (1999). *Stochastic inversion of 3D ERT data* (Doctoral thesis, The University of Arizona, Tucson, AZ).